# Dirac cones in two-dimensional borane

# Dirac cones in two-dimensional borane

Miguel Martinez-Canales,[1,2,*] Timur R. Galeev,[3] Alexander I. Boldyrev,[3] and Chris J. Pickard[2,4,5,†]

[1]*SUPA, School of Physics and Astronomy & EPCC, University of Edinburgh, Peter Guthrie Tait Road, Edinburgh EH9 3FD, United Kingdom*

[2]*Department of Physics and Astronomy, University College London, Gower Street, London WC1E 6BT, United Kingdom*

[3]*Department of Chemistry and Biochemistry, Utah State University, Old Main Hill 0300, Logan, Utah 84322-0300, USA*

[4]*London Institute for Mathematical Sciences, 35a South Street, Mayfair, London W1K 2XF, United Kingdom*

[5]*Department of Materials Science and Metallurgy, University of Cambridge, 27 Charles Babbage Road, Cambridge CB3 0FS, United Kingdom*

(Received 26 September 2012; revised manuscript received 9 October 2017; published 30 November 2017)

We introduce two-dimensional borane, a single-layered material of BH stoichiometry, with promising electronic properties. We show that, according to density functional theory calculations, two-dimensional borane is semimetallic, with two symmetry-related Dirac cones meeting right at the Fermi energy $E_f$. The curvature of the cones is lower than in graphene, thus closer to the ideal linear dispersion. Its structure, formed by a puckered trigonal boron network with hydrogen atoms connected to each boron atom, can be understood as distorted, hydrogenated borophene [Mannix *et al.*, Science **350**, 1513 (2015)]. Chemical bonding analysis reveals the boron layer in the network being bound by delocalized four-center two-electron $\sigma$ bonds. Finally, we suggest high pressure could be a feasible route to synthesize two-dimensional borane.

DOI: 10.1103/PhysRevB.96.195442

The discovery of graphene [1,2], the thinnest, one-atom-thick, planar carbon material, has fueled interest in other reduced dimensionality systems which may have emerging properties. Carbon's close neighbor, boron, is also known to form honeycomb layers, as part of the graphitelike structure of the high-temperature superconductor $MgB_2$ [3]. Here, boron atoms acquire an electronic configuration similar to that of carbon thanks to the electrons donated by interlayer magnesium atoms. In fact, boron showcases a rich variety of bonding, from covalent to delocalized multicenter bonds.

Theoretical interest in all-boron 2D structures has existed for a while; see Refs. [4–11], to cite but a few. The hexagonal $\alpha$ sheet proposed by Tang and Ismail-Beigi [6] was thought to be the most stable 2D allotrope of boron. However, recent work has challenged this: first, Wu *et al.* showed that the $\alpha$ layer was dynamically unstable [12]. Then, Zhou and collaborators found a low-dimensionality allotrope of considerably lower energy [13]. The synthesis of atomically thin boron allotropes has proven challenging. But eventually, Mannix and co-workers [14] reported last year the growth of borophene, a 2D allotrope of boron, on a silver substrate. Against predictions [13], borophene was found to be a highly anisotropic metal. Very recently, Feng and collaborators reported experimental evidence of Dirac fermions in borophene [15].

Much effort has been devoted to design and manufacture materials with graphenelike properties, especially on group-IV systems such as graphyne [16] and silicene [17,18]. $Bi_{1-x}Sb_x$ thin films have also seen active research [19]. Attempts to control the electric properties of such layers has led to the research of hydrogenated layers, such as graphane [20]. Graphane is a fully saturated hydrocarbon, with carbon forming an $sp^3$ bonded buckled honeycomb network. Elias *et al.* have reported the synthesis of graphane by reversible hydrogenation of graphene [21], but the efficiency of this method is contested [22].

One may wonder what properties a hypothetical hydrogenated boron layer will exhibit. It is not unreasonable to expect such layer to be semimetallic or insulating, as two electrons might form a B-H $\sigma$ bond. In order to answer this question, we have performed structure search on volume-restricted boron hydride, in order to focus on low-dimensionality systems. We present an analysis of a particularly stable layered two-dimensional BH structure, which we have identified from a structure search consisting of many thousands of individual samples. Compound searches were restricted to $(BH)_x$ stoichiometry, because this results in high hydrogenation while allowing for a fully bonded boron network.

Based on our searches, we introduce a two-dimensional (2D) borane phase, with the formula BH, which we shall henceforth call 2D borane. We have computed the structural, electronic, and vibrational characteristics of this material, characterized by the crystal structure in Table I.

The search for low-enthalpy $(BH)_x$ stoichiometry 2D structures was performed using *ab initio* random structure searching (AIRSS) [23,24] at the density functional theory (DFT) level. This technique has been successfully applied to a series of H-based systems, such as hydrogen [25,26], silane [23], water ice [27], and ammonia monohydrate [28]. We performed the searches with the CASTEP [29] plane-wave basis set DFT code and the Perdew-Burke-Ernzerhof (PBE) [30] generalized gradient approximation (GGA) density functional and ultrasoft pseudopotentials [31]. We complemented the search results with structures taken from the Inorganic Crystal Structure Database (ICSSD) [32]. The stability of the best candidate structures has been analyzed by computing the phonon dispersion spectra using density functional perturbation theory (DFPT) [33] as implemented in QUANTUM-ESPRESSO [34]. This code was also used for the Berry phase calculations and the symmetry analysis. These calculations used frozen-core PAW potentials [35].

*miguel.martinez@ed.ac.uk

†cjp20@cam.ac.uk

 

TABLE I. Structural parameters of 2D borane ($Pbcm$ symmetry). The long edge has been chosen to minimize layer interactions. The vacuum along the $X$ axis is imposed by the standard crystallographic setting. The layered $Ibam$ phase is recovered by adding a centering at $(\frac{1}{2},\frac{1}{2},\frac{1}{2})$, and $a = 10.669$ Å.

| $a = 10.00$ Å, $b = 3.3662$ Å, $c = 3.0298$ Å | | $\alpha = \beta = \gamma = 90.0^\circ$ |
|---|---|---|
| Atom | Orbit | Fractional coordinates |
| B | 4$d$ | (0.4554 0.4027 0.25) |
| H | 4$d$ | (0.6599 0.5110 0.75) |

Additional technical details concerning the structure searches and other calculations can be found in the Supplemental Material [36], and the relevant calculation data are accessible in Ref. [37].

Solid-state adaptive natural density partitioning (SSAdNDP) [38] was used to analyze chemical bonding. SSAdNDP is a method to interpret bonding in periodic lattices in chemically intuitive terms such as Lewis-type lone pairs and two-center bonds, as well as multicenter delocalized bonds. It is an extension of the AdNDP algorithm [39] to periodic systems and as such was derived from a recently introduced periodic implementation [40] of the natural bond orbital (NBO) analysis [41–44]. A more detailed description of the algorithm may be found elsewhere [38]. A plane-wave DFT calculation was performed using VASP 4.6 [45], using the PAW PBE pseudopotentials [46], summing over a $3 \times 11 \times 11$ $k$-point Monkhorst-Pack grid [47]. A projection algorithm [40] was used to obtain the representation of the PW DFT results in the 6-31$G(dp)$ AO basis set prior to performing the SSAdNDP analysis. VESTA [48] was used for visualizations.

A particularly stable layered structure found for the BH stoichiometry consisted of weakly interacting 2D borane layers. Each layer can be seen as a puckered trigonal boron network with a hydrogen atom connected to each boron atom. The H atoms are located on both sides of the boron layer, and arranged in an alternating zigzag fashion. The multilayer system has $Ibam$ symmetry, while 2D borane itself belongs to the $Pbam$ tile group. 2D borane is displayed in Fig. 1. By removing the other 2D borane layer and relaxing the structure along the plane, we have checked that the single layer system is mechanically stable, while its energetics change by less than 1 meV/atom. It should be noted that the actual boron network is a slight distortion from the already synthesised borophene [14]. This increases our confidence in the feasibility of this material.

The B-B lengths are 1.83–1.91 Å, appreciably longer than the B-B bond predicted for the $\alpha$ sheet (1.67 Å), but in line with those of $Pmmm$ boron [13]. This is due to the fact that fewer electrons participate in the bonding between boron atoms (one electron per boron atom is now used for the formation of the B-H bond). The B-H bonds are 1.19 Å, which is close to the average B-H distance found in boron hydrides and their derivatives [49]. Hydrogenation of graphene to graphane leads to distortion of the carbon network from planarity, but the connectivity between atoms in the hexagons is preserved. The network of boron atoms in 2D borane is however completely rearranged compared to that of either the $\alpha$ sheet, $Pmmm$ or $Pmmn$ boron [13]. Like the latter, 2D borane has no regular vacancy pattern, a feature that is thought to be key to stabilize 2D boron networks [10]. We emphasize, again, that the puckered hexagon arrangement is very similar to that of borophene [14].

The goal of the SSAdNDP analysis is to obtain a bonding pattern with the most localized bonds having occupancies close to two electrons and consistent with the symmetry of the system. Thus, the search is first performed for lone pairs (one center two electron, 1$c$-2$e$, bonds), followed by 2$c$-2$e$, 3$c$-2$e$ $\cdots$ $nc$-2$e$ bonds until the number of revealed bonds equals the number of electron pairs per unit cell. SSAdNDP search revealed no lone pairs in 2D borane. As expected, covalent 2$c$-2$e$ $\sigma$ bonds between hydrogen and boron atoms were found with occupation numbers (ONs) 1.91 $|e|$, close to the ideal 2.00 $|e|$. The search revealed no 3$c$-2$e$ bonds. Instead, 4$c$-2$e$ $\sigma$ bonds connecting boron atoms were found with ON 1.93 $|e|$. Thus, the four 2$c$-2$e$ and four 4$c$-2$e$ bonds revealed per unit cell account for all eight electron pairs and no other bonding elements can be found in 2D borane. Our analysis does not support the presence of $\pi$ bonds in the system. The results of the SSAdNDP chemical bonding analysis are shown in Fig. 1(b).

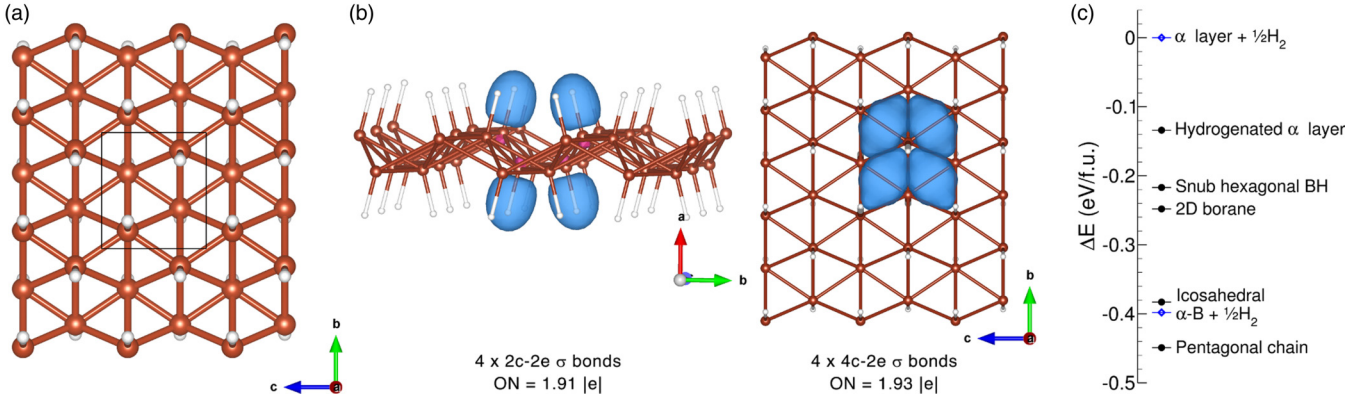


FIG. 1. (a) Structure of the proposed 2D borane. The boron atoms are in red and the hydrogen atoms are in gray. The unit cell is shown in black. (b) SSAdNDP chemical bonding pattern in 2D borane: four 2$c$-2$e$ B-H $\sigma$ bonds and four 4$c$-2$e$ $\sigma$ revealed per unit cell. (c) Energies of selected borane phases, using $\alpha$ layer $+\frac{1}{2}H_2$ as the reference.

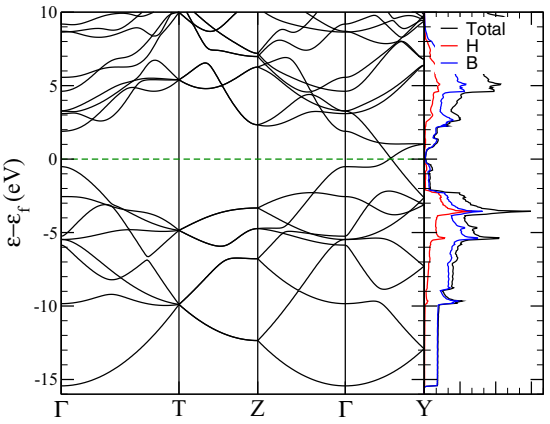


FIG. 2. Band structure and density of states (DOS) of the single-layer 2D borane. The DOS has been computed using OptaDOS [50].

We have calculated and analyzed the band structure and density of states (DOS) of 2D borane, shown in Fig. 2. Shown in Fig. 2, the valence and conduction bands approach smooth-sided cones meeting at the Fermi energy $E_f$. We ruled out the possibility of additional symmetry-inequivalent cones, or a more complex band architecture, by computing the Fermi line of 2D borane [36]. Additionally, a plot of energy isosurfaces of the valence and conduction bands shows two equivalent mirrored elliptic cones near $E_f$ [36]. There is no other state near $E_f$. The conduction and valence bands only meet at $\mathbf{k}_d = \pm 0.2885\mathbf{b}_2$, where $\mathbf{b}_i$ represent the reciprocal-lattice vectors. In contrast, the all-boron $\alpha$ sheet is clearly metallic [8].

The band structure of 2D borane is related to that of 6,6,12-graphyne and *Pmmn* boron atom derivatives [13,16]: a cone is located not at the zone boundary, but along a high-symmetry line. The symmetry of the point ($m2$ or $mm$, compared to $6m$ in graphene) can result in directional electrical properties. The slopes of the cone along $\Gamma Y$ are $+25$ and $-47$ eV Å, and the second derivatives are 21 and 42 eV Å$^2$ respectively. Perpendicularly from $\Gamma Y$, the slope and second derivative are $\pm 52$eV Å and 36 eV Å$^2$ respectively. While the slopes are similar to those of graphene (34 eV Å), the curvatures are about four times smaller. These curvatures are also over an order of magnitude smaller than those of graphynes. These values are very promising, and so could tempt one to say that the DFT band structure of 2D borane near $\mathbf{k}_d$ is a more ideal cone than graphene itself.

It is important to understand the nature of the Dirac cone in 2D borane. In contrast to graphene, the degeneracy at $E_f$ is not entirely dictated by symmetry; it is accidental in the group theory sense. However, it is possible to build an effective Hamiltonian around $E_f$ and $\mathbf{k}_d$. From the symmetry of *Pbcm* borane and the position of $\mathbf{k}_d$, we have a rectangular lattice with mirror plane and two-axis symmetry at $\mathbf{k}_d$. Van Miert and Smith showed that [51], in such cases, the effective Hamiltonian

$$H = \sum_k g(k)(s_k^\dagger s_k - p_k^\dagger p_k) + \sum_k h(k) s_k^\dagger p_k + \text{H.c.}$$

can be applied to model Dirac cone physics near $E_f$, with $g(k_y,k_z) = \epsilon_0 + V_{nn,y}\cos k_y + V_{nn,z}\cos k_z$ and $h(k_y,k_z) = iV_{sp}\sin(k_z)$. We note that such an effective Hamiltonian must be built with bands of strong Boron character, disentangling the effects of hydrogenlike hybridization. A projection of the character of the bands on atomic $s$ and $p$ orbitals is shown in the Supplemental Material. Building an effective tight-binding Hamiltonian that accurately reproduces the borane bands is complicated by coupling between the BH $\sigma$-like valence band and the Boron $p_x$-like band. Therefore, a realistic Hamiltonian would require resorting to, at least, a three-band model. The chirality of $\mathbf{k}_d$ is also displayed in a nontrivial Berry phase of $\pi$ on a path that encloses only one cone. Again, since this effective Hamiltonian describes the only states near $E_f$, transport properties will be dictated by the cone.

We will now show the cone to be resilient. Far from $\mathbf{k}_d$, the closest state to $E_f$ lies at $\Gamma$, about 0.5 eV below. There must be eight full bands below $E_f$, and symmetry imposes $E(\mathbf{k}_d) = E(-\mathbf{k}_d)$. Thus, only perturbations able to shift $E(\Gamma)$ by over 0.5 eV are going to move the cone away from $E_f$. We tested this with symmetry-preserving H displacements: the cone remains at $E_f$ for displacements as large as $\pm 0.1$ Å (8% of the bond length). Moreover, isostructural BF displays a qualitatively identical band structure, with a single symmetry-independent Dirac cone at $E_f$. So does $B_2HF$, as long as the mirror plane symmetry is conserved [36]. Analyzing the symmetry of bands as shown by Bradlyn *et al.* [52] shows the system must be, at the very least, a semimetal: the doubly degenerate $Y_4$ state subduces into two bands of character $A_2$ and $B_2$. At $\Gamma$, the closest levels in energy are $\Gamma_4$ (5.5 eV below $E_f$) and $\Gamma_{11}$ (3.2 eV above $E_f$). $\Gamma_4$ is the only symmetry-compatible state in the first 24 Kohn-Sham states. Band structure plots from molecular dynamics snapshot positions also show the cone persists, except for a small anticrossing gap of about $\sim k_B T$ caused by the instantaneous loss of symmetry.

In order to better understand the states that may form this effective Hamiltonian, we have probed the states in bands 8 and 9 for $\mathbf{k} = \mathbf{k}_d + \delta\mathbf{k}$ for small $|\delta\mathbf{k}|$. The highest occupied molecular orbital (HOMO) and lowest unoccupied molecular orbital (LUMO) states when $\delta\mathbf{k} \| \mathbf{b}_3$ are two mirrored zigzag chains along the diagonal B-B directions. As $\delta\mathbf{k}$ rotates around the cone, the HOMO and LUMO charge densities are consistent with a linear combination of the original zigzag states. Figure 3 shows a detail of the band structure near $\mathbf{k}_d$, as well as the respective HOMO and LUMO charge densities. In an effective Dirac Hamiltonian, the hopping operator would transfer electrons from one set of zigzag chain to the mirrored one. One important difference with symmetry-related crossings is that the pseudospin states must have different symmetry characters. If the characters were the same, the resultant band anticrossing would turn the system into a small gap semiconductor. One peculiar feature of 2D borane is the mobility of the cone: $\mathbf{k}_d$ is allowed to move along $\Gamma Y$, and does so when compressed or strained. This opens up the possibility of tuning the position of $\mathbf{k}_d$.

We have tested the dynamical stability of 2D borane, and found no unstable phonon modes exist in the Brillouin zone. Additionally, the lattice dynamics of the multilayered *Ibam* borane have also been confirmed to be stable. The relevant phonon dispersion curves and the details of the

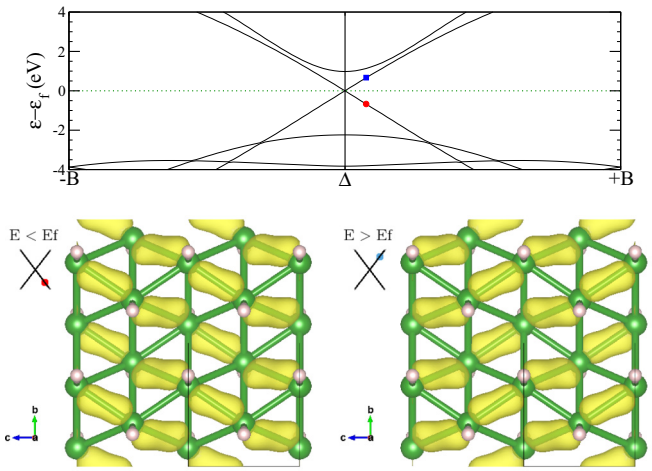


FIG. 3. Top: Detail of the band structure of 2D borane, passing through $\mathbf{k_d}$ and perpendicular to $\Gamma Y$. Bottom: Charge densities associated with the highlighted $k$ points in the band structure.

calculations can be found in the Supplemental Material [36]. 2D borane displays a quadratic acoustic mode responsible for the layer ripples in the long-wavelength limit. As in graphene, ripples should appear on 2D borane. The structure of the layer is not strictly two dimensional, and ripples may not play a pivotal role on the stability of 2D borane. Finite-temperature and anharmonic effects do not destabilize 2D borane: we have performed molecular dynamics simulations for 3 ps at 300 K, in $6 \times 6$ supercells and with 1 fs time step [36]. 2D borane remained stable throughout the simulation. Finally, the phonon spectra of 2D borane and *Ibam* borane are essentially identical. This indicates a very weak interaction between layers. Should the *Ibam* borane be synthesized, exfoliation will be a viable mechanism to obtain 2D borane.

The energetics of 2D borane and other BH compounds have also been analyzed, and the results are shown in Fig. 1(c). Of all the various layered BH compounds analyzed, 2D borane had the lowest enthalpy. Overall, the lowest energy structure we found in our searches is a ribbon of buckled pentagonal tiles, about 200 meV/BH more stable than our layered phase. The best molecular structure was a cubic arrangement of $B_{12}H_{12}$ icosahedra. This system is very charge deficient and as such has only been observed in nature as a doubly charged anion, either as a part of a salt or in solution [53]. The crystal structures of these systems can be found in the Supplemental Material [36].

The large hydrogen content of 2D borane makes it a candidate for hydrogen storage, and so we compared the energetics of borane with the segregated phases. As seen in Fig. 1, 2D borane, as well as some other layerings, are more stable than $\alpha$-layer B $+\frac{1}{2}H_2$. In order to find the best candidate for the hydrogenated $\alpha$ layer we performed some additional directed searching [36]. However, the best fully hydrogenated $\alpha$ layer we found has a higher energy than $\alpha$-layer $+\frac{1}{2}H_2$, and thus higher than 2D borane too. We also found a hydrogenated analog of the snub boron sheet predicted by Zope and Baruah [9]. It is, however, 32 meV/formula unit less stable than 2D borane. We have computed the full $B_xH_y$ hull, including large experimental phases of various stoichiometries, as seen in the Supplemental Material [36]. We found molecular diborane ($B_2H_6$) not to be a thermodynamically stable stoichiometry. At the PBE level, the only stable stoichiometry was $B_9H_{11}$. We note the stable phase is formed by boron-defective icosahedra. As expected, 2D borane would decompose, but not into diborane plus $\alpha$ layer. In the layered case, the reaction

$$\text{2D borane} \rightarrow \alpha \text{ layer} + \tfrac{1}{2}H_2$$

requires an energy of 0.496 eV/$H_2$. It is in the 0.2–0.6-eV range, the optimal binding energy for an ambient conditions hydrogen storage material [54,55].

As a final remark, a paper on boron hydrides under pressure, published during the review process, reported the stabilization of the BH stoichiometry [56]. Hu *et al.* independently also found the multilayered *Ibam* phase, which they report to become the stable BH structure under pressure. This suggests that high-pressure synthesis of *Ibam* BH, followed by exfoliation, is a plausible mechanism for the synthesis of 2D borane.

In conclusion, in this work we introduce 2D borane, a single-layered BH material. It is the most stable layered phase found in our structure searches. The energetics show 2D borane is stable towards decomposition to $\alpha$-layer $+\frac{1}{2}H_2$. It is formed by a puckered triangular boron network, in which hydrogen atoms connect to each boron site from alternating sides of the network, forming zigzaglike chains. The band structure and density of states of 2D borane show two symmetry related smooth-sided cones with the Dirac points right at the Fermi energy. The cone structure is protected by the electron counting sum rule and is located along a high-symmetry line. As a result, it can move along $\Gamma Y$. 2D borane also shows remarkably small curvatures even in symmetry-unrestricted directions, suggesting this material may have graphenelike electronic properties. The SSAdNDP analysis revealed that the boron atoms are bonded by delocalized $4c$-$2e$ $\sigma$ bonds. We hope that our work will motivate an experimental search for this material.

C.J.P. and M.M.C. acknowledge financial support from EPSRC Grants No. EP/K013688/1 and No. EP/G007489/2 (UK) and the use of the UCL Legion High Performance Computing Facility as well as HECToR and Archer, the UK's national high-performance computing services. C.J.P. further acknowledges Department of the Navy Grant No. N62909-12-1-7109, issued by the Office of Naval Research Global. The work at USU was supported by National Science Foundation (Grant No. CHE-1664379). Computing, storage, and other resources from the Division of Research Computing in the Office of Research and Graduate Studies at Utah State University and the support and resources from the Center for High Performance Computing at the University of Utah are gratefully acknowledged.

[1] K. S. Novoselov, A. K. Geim, S. V. Morozov, D. Jiang, Y. Zhang, S. V. Dubonos, I. V. Grigorieva, and A. A. Firsov, Science **306**, 666 (2004).

[2] K. S. Novoselov, A. K. Geim, S. V. Morozov,, D. Jiang, M. I. Katsnelson, I. V. Grigorieva, S. V. Dubonos, and A. A. Firsov, Nature (London) **438**, 197 (2005).

[3] J. Nagamatsu, N. Nakagawa, T. Muranaka, Y. Zenitani, and J. Akimitsu, Nature (London) **410**, 63 (2001).

[4] I. Boustani, A. Quandt, E. Hernández, and A. Rubio, J. Chem. Phys. **110**, 3176 (1999).

[5] M. H. Evans, J. D. Joannopoulos, and S. T. Pantelides, Phys. Rev. B **72**, 045434 (2005).

[6] H. Tang and S. Ismail-Beigi, Phys. Rev. Lett. **99**, 115501 (2007).

[7] H. Tang and S. Ismail-Beigi, Phys. Rev. B **80**, 134113 (2009).

[8] X. Yang, Y. Ding, and J. Ni, Phys. Rev. B **77**, 041402 (2008).

[9] R. Z. Zope and T. Baruah, Chem. Phys. Lett. **501**, 193 (2011).

[10] E. S. Penev, S. Bhowmick, A. Sadrzadeh, and B. I. Yakobson, Nano Lett. **12**, 2441 (2012).

[11] X. Yu, L. Li, X.-W. Xu, and C.-C. Tang, J. Phys. Chem. C **116**, 20075 (2012).

[12] X. Wu, J. Dai, Y. Zhao, Z. Zhuo, J. Yang, and X. C. Zeng, ACS Nano **6**, 7443 (2012).

[13] X.-F. Zhou, X. Dong, A. R. Oganov, Q. Zhu, Y. Tian, and H.-T. Wang, Phys. Rev. Lett. **112**, 085502 (2014).

[14] A. J. Mannix, X.-F. Zhou, B. Kiraly, J. D. Wood, D. Alducin, B. D. Myers, X. Liu, B. L. Fisher, U. Santiago, J. R. Guest, M. J. Yacaman, A. Ponce, A. R. Oganov, M. C. Hersam, and N. P. Guisinger, Science **350**, 1513 (2015).

[15] B. Feng, O. Sugino, R.-Y. Liu, J. Zhang, R. Yukawa, M. Kawamura, T. Iimori, H. Kim, Y. Hasegawa, H. Li, L. Chen, K. Wu, H. Kumigashira, F. Komori, T.-C. Chiang, S. Meng, and I. Matsuda, Phys. Rev. Lett. **118**, 096401 (2017).

[16] D. Malko, C. Neiss, F. Viñes, and A. Görling, Phys. Rev. Lett. **108**, 086804 (2012).

[17] S. Lebègue and O. Eriksson, Phys. Rev. B **79**, 115409 (2009).

[18] P. Vogt, P. De Padova, C. Quaresima, J. Avila, E. Frantzeskakis, M. C. Asensio, A. Resta, B. Ealet, and G. Le Lay, Phys. Rev. Lett. **108**, 155501 (2012).

[19] S. Tang and M. S. Dresselhaus, Nano Lett. **12**, 2021 (2012).

[20] J. O. Sofo, A. S. Chaudhari, and G. D. Barber, Phys. Rev. B **75**, 153401 (2007).

[21] D. C. Elias, R. R. Nair, T. M. G. Mohiuddin, S. V. Morozov, P. Blake, M. P. Halsall, A. C. Ferrari, D. W. Boukhvalov, M. I. Katsnelson, A. K. Geim, and K. S. Novoselov, Science **323**, 610 (2009).

[22] H. L. Poh, F. Sanek, Z. Sofer, and M. Pumera, Nanoscale **4**, 7006 (2012).

[23] C. J. Pickard and R. J. Needs, Phys. Rev. Lett. **97**, 045504 (2006).

[24] C. J. Pickard and R. J. Needs, J. Phys.: Condens. Matter **23**, 053201 (2011).

[25] C. J. Pickard and R. J. Needs, Nat. Phys. **3**, 473 (2007).

[26] C. J. Pickard, M. Martinez-Canales, and R. J. Needs, Phys. Rev. B **85**, 214114 (2012).

[27] C. J. Pickard, M. Martinez-Canales, and R. J. Needs, Phys. Rev. Lett. **110**, 245701 (2013).

[28] A. D. Fortes, E. Suard, M.-H. Lemée-Cailleau, C. J. Pickard, and R. J. Needs, J. Am. Chem. Soc. **131**, 13508 (2009).

[29] S. J. Clark, M. D. Segall, C. J. Pickard, P. J. Hasnip, M. J. Probert, K. Refson, and M. C. Payne, Z. Kristallogr. **220**, 567 (2005).

[30] J. P. Perdew, K. Burke, and M. Ernzerhof, Phys. Rev. Lett. **77**, 3865 (1996).

[31] D. Vanderbilt, Phys. Rev. B **41**, 7892 (1990).

[32] Inorganic crystal structure database, http://www.fiz-karlsruhe.de/icsd.html.

[33] S. Baroni, S. de Gironcoli, A. Dal Corso, and P. Giannozzi, Rev. Mod. Phys. **73**, 515 (2001).

[34] P. Giannozzi, S. Baroni, N. Bonini, M. Calandra, R. Car, C. Cavazzoni, D. Ceresoli, G. L. Chiarotti, M. Cococcioni, I. Dabo, A. Dal Corso, S. de Gironcoli, S. Fabris, G. Fratesi, R. Gebauer, U. Gerstmann, C. Gougoussis, A. Kokalj, M. Lazzeri, L. Martin-Samos *et al.*, J. Phys.: Condens. Matter **21**, 395502 (2009).

[35] P. E. Blöchl, Phys. Rev. B **50**, 17953 (1994).

[36] See Supplemental Material at http://link.aps.org/supplemental/10.1103/PhysRevB.96.195442 for information on the band structures, lattice dynamics, molecular dynamics, and a symmetry analysis of the bands.

[37] M. Martinez-Canales, T. Galeev, A. Boldyrev, and C. Pickard, Dirac cones in two-dimensional borane, 2012-2017 [dataset]. University of Edinburgh, School of Physics and Astronomy, https://datashare.is.ed.ac.uk/handle/10283/2949.

[38] T. R. Galeev, B. D. Dunnington, J. R. Schmidt, and A. I. Boldyrev, Phys. Chem. Chem. Phys. **15**, 5022 (2013).

[39] D. Y. Zubarev and A. I. Boldyrev, Phys. Chem. Chem. Phys. **10**, 5207 (2008).

[40] B. D. Dunnington and J. R. Schmidt, J. Chem. Theory Comput. **8**, 1902 (2012).

[41] J. P. Foster and F. Weinhold, J. Am. Chem. Soc. **102**, 7211 (1980).

[42] A. E. Reed, R. B. Weinstock, and F. Weinhold, J. Chem. Phys. **83**, 735 (1985).

[43] A. E. Reed, L. A. Curtiss, and F. Weinhold, Chem. Rev. **88**, 899 (1988).

[44] F. Weinhold and C. Landis, *Valency and Bonding. A Natural Bond Orbital Donor-Acceptor Perspective* (Cambridge University Press, Cambridge, UK, 2005).

[45] G. Kresse and J. Furthmüller, Comput. Mater. Sci. **6**, 15 (1996).

[46] G. Kresse and D. Joubert, Phys. Rev. B **59**, 1758 (1999).

[47] H. J. Monkhorst and J. D. Pack, Phys. Rev. B **13**, 5188 (1976).

[48] K. Momma and F. Izumi, J. Appl. Crystallogr. **44**, 1272 (2011).

[49] W. N. Lipscomb, *Boron Hydrides* (Benjamin, New York, 1963).

[50] A. J. Morris, R. J. Nicholls, C. J. Pickard, and J. R. Yates, Comput. Phys. Commun. **185**, 1477 (2014).

[51] G. van Miert and C. M. Smith, Phys. Rev. B **93**, 035401 (2016).

[52] B. Bradlyn, L. Elcoro, J. Cano, M. G. Vergniory, Z. Wang, C. Felser, M. I. Aroyo, and B. A. Bernevig, Nature (London) **547**, 298 (2017).

[53] A. R. Pitochelli and F. M. Hawthorne, J. Am. Chem. Soc. **82**, 3228 (1960).

[54] Y.-H. Kim, Y. Zhao, A. Williamson, M. J. Heben, and S. B. Zhang, Phys. Rev. Lett. **96**, 016102 (2006).

[55] P. B. Sorokin, H. Lee, L. Y. Antipina, A. K. Singh, and B. I. Yakobson, Nano Lett. **11**, 2660 (2011).

[56] C.-H. Hu, A. R. Oganov, Q. Zhu, G.-R. Qian, G. Frapper, A. O. Lyakhov, and H.-Y. Zhou, Phys. Rev. Lett. **110**, 165504 (2013).